Silicon (2022) 14:11147–11161
https://doi.org/10.1007/s12633-022-01842-0

ORIGINAL PAPER

Superior Surface Protection, Mechanical and Hydrophobic Properties of Silanized Tungsten Carbide Nanoparticles Encapsulated Epoxy Nanocomposite Coated Steel Structures in Marine Environment

Joseph Raj Xavier[1]

Received: 14 December 2021 / Accepted: 21 March 2022 / Published online: 5 April 2022

Abstract

The influence of 3-mercaptopropyltrimethoxysilane (MPTMS)/WC nanoparticles within the neat epoxy (EP) coated mild steel was investigated for its hydrophobic, mechanical and electrochemical properties in the marine environment. The MPTMS modified WC nanoparticles were confirmed by TGA, XRD, SEM/EDX, AFM and TEM to investigate the chemical structure. The electrochemical techniques (EIS, SECM and Polarization) were utilized to investigate the protective properties of the investigated coatings. The FE-SEM/EDX and XRD were carried out to examine the nature of the corrosion products. The water repellent property of EP, EP/WC, EP/MPTMS, and EP-MPTMS/WC coatings was characterized by contact angle measurement (CA). It was found that the coating resistance of the EP-MPTMS/WC nanocomposite is over 41% higher than that of the pure epoxy coating. The coating resistance of the EP-MPTMS/WC coated steel was found to be 5699.76 kΩ.cm^2 whereas the coating resistance of EP was 1.11 kΩ.cm^2 even after 240 h exposed to the marine environment. Similarly, the corrosion current density of the EP-MPTMS/WC nanocomposite coated steel obtained by SECM technique was 2.1 nA/cm^2 in comparison to EP coated steel (14.4 nA/cm^2). The results showed that the newly developed EP-MPTMS/WC nanocomposite coating possessed superior corrosion protection and enhanced hydrophobic behaviors (WCA: 144°). The investigated coatings showed profound mechanical properties. Therefore, the compatibility of EP, MPTMS and WC nanoparticles was established by superior hydrophobicity and improved corrosion protection and enhanced mechanical properties.

Keywords Silanes · Functional materials · WC · Nanocomposite coatings · SECM

1 Introduction

Metals and its alloys are widely used in a variety of applications such as industrial equipment, construction materials, electric and electronic equipments, pipeline industries, desalination plants, cooling water systems, pharmaceuticals, etc. [1–3]. However, when the metals are exposed to the corrosive environments, they undergo degradation due to their thermodynamic instability. Billions of dollars per year worldwide are wasted due to metallic. The coating is widely applied to the metals/alloys to prevent corrosion when they are exposed to harsh environments. It is extensively used because the penetration of corrosive ions through the coating films is prevented so that the life span of the materials is prolonged. Water based polymers such as acrylic [4], polyurethane (PU) [5], alkyd [6], epoxy [7], polyester [8] etc., and their combinations are extensively used as the coating films due to their popularity and complementary performance.

Epoxy possesses good durability and excellent resistance properties among different polymers. It acts against thermal and chemical degradation [9–11]. Although the epoxy resins show excellent anticorrosion, good chemical properties, and improved adhesive properties [12, 13], their poor outdoor durability is the cause of concern. Therefore, epoxy hybrids are used extensively in all the industrial sectors. However, the presence of micro-voids in the polymers results in hydrophilicity which leads to the degradation of the coatings [14, 15]. The pores in the polymer help the corrosive ions to penetrate through the interface of the coating-metal. The number of investigations has been carried out to enhance the polymer properties [16, 17].

✉ Joseph Raj Xavier
drjosephrajxavier@gmail.com

[1] Department of Chemistry, Saveetha School of Engineering, Saveetha Institute of Medical and Technical Sciences, Chennai, Tamil Nadu 602 105, India

In order to increase the barrier properties of the polymers, nanoparticles are introduced to the coating formulations recently. When nano-sized particles are added to the polymers, they help to fill up the pores and cracks present in the coatings and reduce the degradation of the coated materials and increase the barrier properties [18]. Moreover, the inorganic nanoparticles increase the cross-linking structures which minimize the pores in the coating formulations [19]. The improved mechanical and barrier properties were found by incorporating nano-fillers in the polymers [20, 21]. Nano-fillers slow down the diffusion of corrosive ions, prevent the ions penetrating through the coating-metal interface and reduce the rate of corrosion of the coated materials [22].

Decreased corrosion resistance of the composite coatings containing nano-fillers occurs because of the low compatibility, poor dispersibility, and agglomeration of nanoparticles in the coating formulations. The silane modified WC nanoparticles were found to reduce agglomeration, increase the interfacial compatibility with epoxy resin [23]. The corrosion resistance of PDMAS/TiO_2/epoxy coating versus unmodified epoxy was investigated by salt spray accelerated corrosion test. The results revealed the excellent barrier properties and good self-healing effect [24]. The incorporation of gallic acid esters transformed WC nanoparticles in the epoxy resins resulted in the increased anticorrosion properties when compared to the pure epoxy coatings [25]. Hence, the addition of the surface modified nanoparticles to the polymers produces better barrier properties [26]. The grafting of surface modified nanoparticles into the polymers increases the dispersibility and compatibility of the nanoparticles. However, the crystalline structure of the nanoparticles has not been changed during the modification processes. The agglomeration of the nano ZnO particles can be reduced drastically by the use of polyvinyl alcohol [27]. Excellent corrosion inhibition efficiency was produced by the EP/PANI/SnO_2 nanocomposites, which helped to protect the steel structures against corrosive environments [28]. The higher corrosion resistant property was displayed by the addition of poly (o-anisidine)/SiC in the epoxy resin [29]. When the SiC nanoparticles interacted with poly (o-ethoxyaniline), improved protection properties were produced in comparison with pure polymer [30]. Similarly, the incorporation of multifunctional nanocomposites resulted in the superior barrier properties of the epoxy resins [31]. Hence, from the literature, it was clear that the inclusion of surface modified nanoparticles into the polymers enhanced the corrosion resistance and hydrophobic properties.

To the best of our knowledge, surface protection, water repellent, and mechanical properties of 3-mercaptopropyltrimethoxysilane (MPTMS) modified WC nanoparticles in epoxy have not been reported for mild steel. Therefore, this article presents MPTMS/WC in epoxy matrix as eco-friendly coating materials for mild steel corrosion. The synthesized MPTMS/WC materials were characterized using thermogravimetric analysis (TGA), transmission electron microscopy (TEM), Scanning electron microscope (SEM), Atomic force microscopy (AFM) and X-Ray Diffraction (XRD) techniques. Electrochemical methods such as EIS, polarization, and SECM were utilized for the investigation of the barrier properties of the coated surface. The corrosion products were examined by FE-SEM/EDX and XRD techniques. The adhesion and hardness properties of the coated materials were investigated. The wettability of the coatings was studied by contact angle measurements. The permeability of water and oxygen in the coated surface was studied extensively using permeability tests.

2 Experimental

2.1 Chemicals and Reagents

Tungsten carbide (WC), epoxy resin, 3-mercaptopropyltrimethoxysilane (MPTMS), ethanol, and acetone were supplied by Sigma-Aldrich. The mild steel panels consisting of 40 mm × 30 mm × 30 mm were used for the coating. The steel samples were abraded with SiC using different grits and washed with acetone. Analytical grade reagents were used for the investigation as received.

2.2 Preparation of Epoxy-3-Mercaptopropyltrimethoxysilane /WC Nanocomposite

The MPTMS/WC nanoparticles were synthesized when 3 g of 3-mercaptopropyltrimethoxysilane in 60 mL of deionized water was mixed with nanoparticles followed by ultra-sonication. The resultant products were dried by keeping it in an oven at 90 °C for about 5 h to get the MPTMS/WC nanoparticles. Different wt.% of MPTMS/WC nanoparticles were mixed with epoxy and aliphatic amine hardener (3:1 ratio) using a magnetic stirrer (3000 rpm) for 2 h to get stable formulations. The resultant coating formulations were applied on mild steel using draw down process. The prepared coated specimens were investigated by electrochemical techniques for their barrier properties and by mechanical testing for their mechanical properties in natural seawater for 1, 24, 120 and 240 h.

2.3 Characterization of MPTMS/WC Nanoparticles

The surface modification of WC was proved using thermogravimetry analysis (TGA) (Model NETZSCH STA 449 F3 JUPITER). X-ray diffractometer (XRD) (Philips

X'Pert) was utilized to examine WC and modified WC nanoparticles. The scan rate of 0.42°/s was used and the 2θ scans were ranging from $20^o \leq 2\theta \leq 90^o$. The surface morphological studies were carried out for WC and modified WC nanoparticles by FE-SEM/EDX analysis (Model FEI-Quanta FEG 200F). The dispersion of modified WC nanoparticles was confirmed by TEM.

2.4 Electrochemical Techniques

EIS and potentiodynamic polarization studies were carried out for coated specimens with and without exposure to chloride using Potentiostat/galvanostat (Autolab PGSTAT 30, Echo Chemie, B.V. and Netherlands). Three electrode systems consisting of Ag/AgCl (reference), a Pt strip (counter), and the coated specimens (working) were used. The frequency range of 100 kHz to 1 mHz and the potential of 10 mV were utilized to carry out the EIS experiment. The scan rate of 0.1 mV s^{-1} was used in the investigation of coated specimens by potentiodynamic polarization technique. Experimental data were extracted from curve fittings.

SECM (CH-Instruments, Austin, TX, USA) was conducted to analyze the scratched surface of the coated steel specimens in seawater. The Pt microelectrode was utilized as the SECM tip. The piezoelectric motor was used to fix and control the tip movement. The reference, counter and working electrodes were Ag/AgCl, a Pt strip, and coated steel specimens, respectively. The scanning rate of 20 μm s^{-1} was applied. The height of the tip from the coated specimen was fixed as 20 μm.

2.5 Investigation of Degradation Products

The degradation products obtained at the coating-steel interface of the EP, EP-WC, EP-MPTMS, and EP-MPTMS/WC coated mild steel after exposure to chloride media for 240 h were examined by FE-SEM/EDX techniques. Similarly, the degradation products emerged at the coating-steel interface of the EP, EP-WC, EP-MPTMS, and EP-MPTMS/WC coatings exposed to chloride media for 240 h were investigated by XRD equipment with the scan range of $20^o \leq 2\theta \leq 70^o$. The scan rate used for the investigation was 0.42°/s.

2.6 Mechanical Studies

Pull-off adhesion test was performed for the EP, EP-MPTMS, EP-WC and EP-MPTMS/WC coated specimens before and after exposure to chloride media for different days. The pull-off adhesion test was carried out by tensile strength testing machine (Instron). Microhardness test was performed for the EP, EP-MPTMS, EP-WC and EP-MPTMS/WC coated specimens before and after exposed to chloride electrolytes for different days. HM113 Vicker's hardness tester was used for the investigation. The tensile test was carried out for the EP, EP-WC, EP-MPTMS, and EP-MPTMS/WC coated specimens before and after exposure to chloride media for different days using the universal testing machine. Generally, the tests were done in triplicates and the average values were used for the interpretation.

2.7 Permeability of the Coated Specimens

The water permeability in the EP, EP-WC, EP-MPTMS, and EP-MPTMS/WC coated specimens was examined before and after exposing to the electrolytes for different days by a pervaporation test. Similarly, the oxygen permeability in the EP, EP-WC, EP-MPTMS, and EP-MPTMS/WC coated specimens was examined before and after exposure to the chloride media for different days as per ASTM D3985. A coulometric sensor detector was used to detect the diffusing oxygen. The sensor was only sensitive to the oxygen. All the tests were carried out in triplicate and the average values were taken for interpretations.

The contact angle measurements were carried out on the surface of the pure EP, EP-WC, EP-MPTMS, and EP-MPTMS/WC coated specimens. Generally, the water droplets were placed on the coated specimens at different locations and the resultant images were captured using a high powered camera. Measurements were done several times with <1° measurement error.

3 Results and Discussion

3.1 Characterization of MPTMS Modified WC Nanoparticles

3.1.1 TGA

The thermal properties of the WC and MPTMS/WC nanoparticles were investigated by the TGA. The loss of weight curves for the WC and MPTMS/WC nanoparticles were depicted in Fig. 1. Three consecutive weight loss steps are shown by the TGA curve of pure WC nanoparticles. Weight loss of 13% is firstly noticed approximately at 100–150 °C which is correlated to the removal of absorbed molecules such as volatile impurities and H_2O [32]. Secondly, another slight loss of weight after 150 °C is due to the removal of water molecules resulting from the condensation reaction [33]. The 63% loss in weight around 220–350 °C is because of the thermal oxidative degradation. At last, complete decomposition is achieved around 450–800 °C which results in the constant weight of WC nanoparticles.

In the case of MPTMS/WC nanoparticles, weight loss of 6% only is noticed initially at 175 °C. It shows the less weight loss around 0 to 120 °C for the MPTMS/WC nanoparticles.

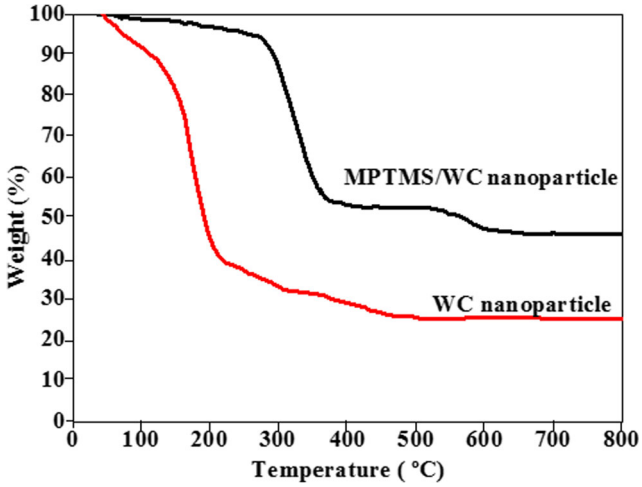

Fig. 1 TGA of WC and 3-mercaptopropyltrimethoxysilane (MPTMS) functionalized WC (MPTMS/WC) nanoparticles

This proves the lesser absorption of water molecules due to the surface modification of WC by MPTMS. Secondly, the weight loss percentage is found to be around 45 at the temperature range of 260–350 °C. This is due to the fact that the MPTMS/WC nanoparticles are thermally decomposed. Finally, only 10% loss of weight is found for the modified WC nanoparticles at 550–650 °C. Therefore, It is confirmed from TGA that the MPTMS/WC nanoparticles are stable thermally even at high temperatures.

3.1.2 X-Ray Diffraction (XRD)

Figure 2 illustrates the XRD patterns of pure WC and MPTMS modified WC samples. The peaks obtained at (2θ) 31.4°, 35.85°, 48.4°, 65.6°, 73.2°, and 87.17° are related to (001), (100), (101), (110), (111), and (201) crystal faces [34]. However, MPTMS/WC nanoparticles display the same peaks as that of the WC nanoparticles but with reduced intensities in their peaks. Therefore, it is concluded from the investigation that the WC nanoparticles are continued to maintain its crystalline structure, even after its surface modification by MPTMS with enriched cross-linked structures. It is also confirmed that the structures of WC nanoparticles are not affected due to its modification.

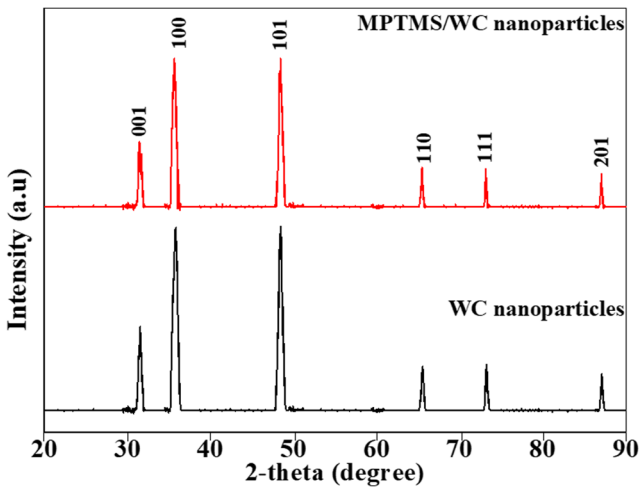

Fig. 2 XRD patterns of WC and 3-mercaptopropyltrimethoxysilane (MPTMS) functionalized WC (MPTMS/WC) nanoparticles

3.1.3 FE-SEM/EDX and TEM Analysis

Figure 3 displays the results of the SEM/EDX analysis of WC and MPTMS/WC nanoparticles. Here, it is seen from the SEM images that MPTMS/WC shows least agglomeration when compared to the pure WC. This is because of good distribution of modified WC by MPTMS in the medium. No other elements except W and C are found during the EDX analysis of WC nanoparticles confirming the purity of the nanoparticles (Fig. 4a). However, along with W and C, Si, S, C, and O elements are also present during the EDX analysis of MPTMS/WC nanoparticles. Therefore, the surface modification of WC nanoparticles by MPTMS is confirmed by the detection of the Si, S, C, O, and W elements in MPTMS/WC nanoparticles.

Figure 4a, b show the TEM images of pure WC and MPTMS/WC nanoparticles, respectively. It is shown from the figures that the MPTMS/WC nanoparticles are well dispersed with nano-sized structures, whereas nano-sized pure WC nanoparticles are agglomerated. It is confirmed from the investigation that the MPTMS/WC nanoparticles are evenly distributed because of the surface modification of WC nanoparticles by MPTMS which help to disperse in the polymer matrix uniformly.

3.2 Electrochemical Studies

3.2.1 Electrochemical Impedance Spectroscopic (EIS) Technique

Figure 5 presents the Nyquist plots of bare mild steel, epoxy (EP), EP with different weight percentage of MPTMS/WC coated mild steel exposed to the marine environment. A Nyquist plot is a parametric plot of a frequency response used in automatic control and signal processing. The most common use of Nyquist plots is for assessing the stability of a system with feedback. It can be interpreted from the plots that the maximum impedance is displayed as the percentage of MPTMS/WC nanoparticles in EP increases up to 2.0 wt.%. However, the impedance starts decreasing when the weight percentage of MPTMS/WC nanoparticles reaches 2.5 wt.%. This could be due to the aggregation of nanoparticles, which result in the decrease of impedance [35]. Therefore, it is proved that 2.0 wt.% MPTMS/WC nanoparticles are considered to be the optimum percentage which could be used for further studies. Figure 6 shows Nyquist plots of pure EP, EP/

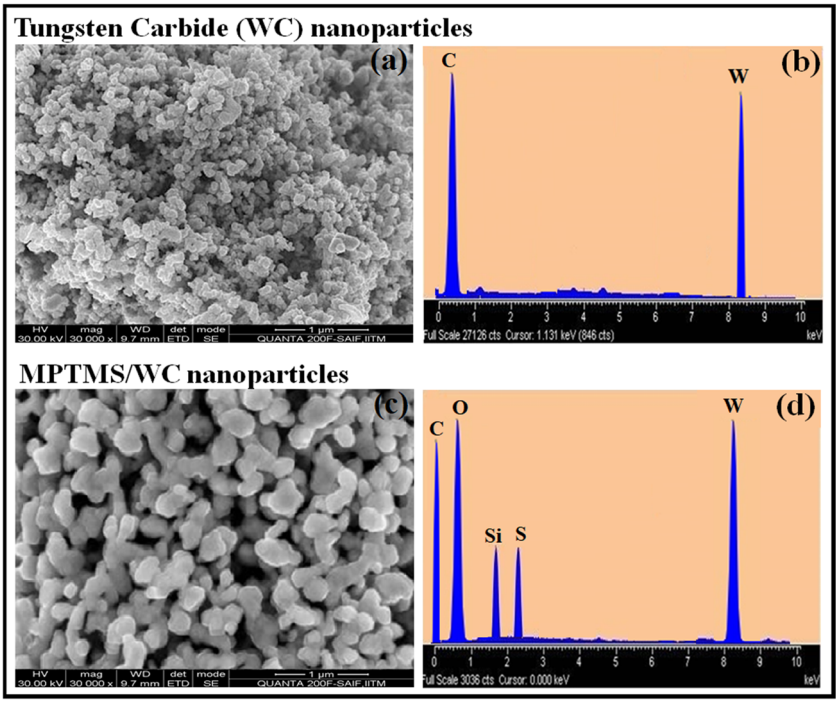

Fig. 3 SEM/EDX analyses of WC and 3-mercaptopropyltrimethoxysilane (MPTMS) functionalized WC (MPTMS/WC) nanoparticles

WC, EP-MPTMS, and EP-MPTMS/WC nanocomposites coated mild steel samples in chloride media for different immersion days (1 to 240 h). The equivalent circuit model used for fitting the plots is shown in Fig. 7.

Table 1 represents electrochemical data generated after curve fittings of uncoated and coated mild steel with EP, EP/WC, EP-MPTMS, and EP-MPTMS/WC nanocomposites for various days of exposure in chloride environments. The pure EP coated specimen shows very low resistances of coating (R_{coat}: 142.35 kΩ.cm^2) as well as charge transfer (R_{ct}: 245.67 kΩ.cm^2) compared to the EP-WC, EP-MPTMS, and EP-MPTMS/WC composite coatings at 1 h exposure to the electrolyte. However, as the exposure time is at 240 h, pure epoxy coated specimen displays drastic decrease in the resistances of coating (1.11 kΩ.cm^2) as well as charge transfer (87.12 kΩ.cm^2) compared to other investigated coatings. This is because of the fact that the rapid penetration of the electrolytes reaching the coating-metal interface causing increased corrosion rate. On the other hand, for the EP-WC coated specimen, the values of R_{coat} (2685.12 kΩ.cm^2) and R_{ct} (2890.46 kΩ.cm^2) are found to be higher when revealed to the electrolyte for 1 h. Moreover, these values are decreased significantly (R_{coat}: 1401.33 kΩ.cm^2; R_{ct}: 1698.75 kΩ.cm^2) when they are exposed to the electrolyte at 240 h. The significant reduction in the resistances of coating and charge transfer is due to the fact that the aggregation of nanoparticles in the EP matrix causes the formation of pores which allow the electrolyte to reach the metal-coating interface quickly permitting the corrosion processes to start immediately.

In the case of the EP-MPTMS coated steel, there is a slight increase in the values of R_{coat} (3056.35 kΩ.cm^2) and R_{ct} (3299.55 kΩ.cm^2) at 1 h. This may be due to the synergistic effect caused by EP and MPTMS, which enhances the bonding strength of the EP-MPTMS coating formulations. This effect causes the electrolyte to reach the interface little longer period. However, in the case of the EP-MPTMS/WC nanocomposite, the values of R_{coat} (5890.65 kΩ.cm^2) and R_{ct} (6998.45 kΩ.cm^2) are found to be even higher when it is in contact with the electrolyte for 1 h. No drastic reduction in the values of the resistances of coating is observed for the EP-MPTMS/WC composites even after revealing to the electrolyte for 240 h. The R_{coat} and R_{ct} values for the EP-MPTMS/WC nanocomposite are found to be slightly decreased (R_{coat}: 5699.76 kΩ.cm^2; R_{ct}: 6754.90 kΩ.cm^2) when the exposure time is more (240 h). The inclusion of surface modified WC nanoparticles by MPTMS in EP matrix helps to cover the pores in the coatings. This leads to torturous pathways for the electrolyte to reach the metal-coating interface. These R_{coat} and R_{ct} values confirm the superior protective properties of the EP-MPTMS/WC composite coatings which help to prolong the life span of the coated specimen even when they are exposed to harsh environments. The addition of MPTMS/WC nanoparticles to the polymer matrix produces the nanocomposites containing increased cross-linking density and strong binding strength which drastically cuts the movement of aggressive ions reaching the interface, thus enhancing the coating resistance of the coated specimen. This avoids the delamination of the coated films, mainly due to synergistic

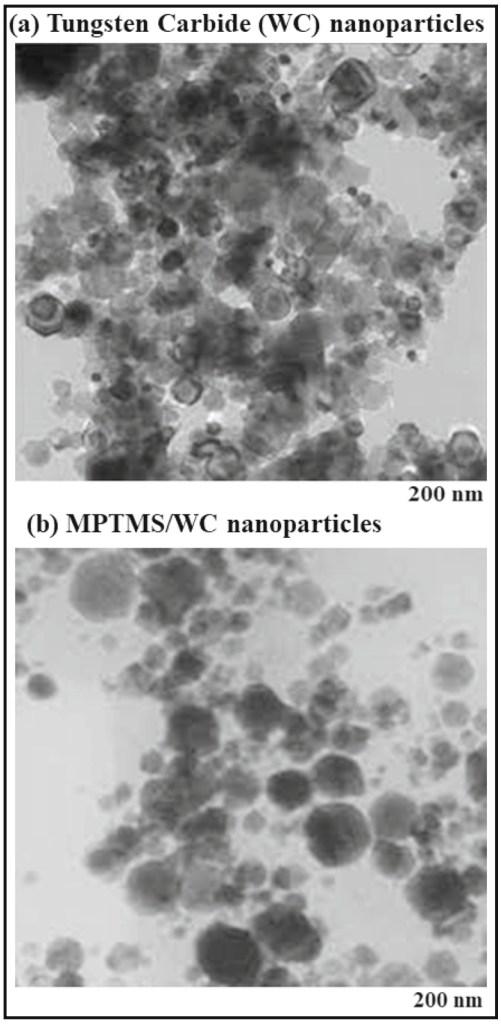

Fig. 4 TEM images of WC and 3-mercaptopropyltrimethoxysilane (MPTMS) functionalized WC (MPTMS/WC) nanoparticles

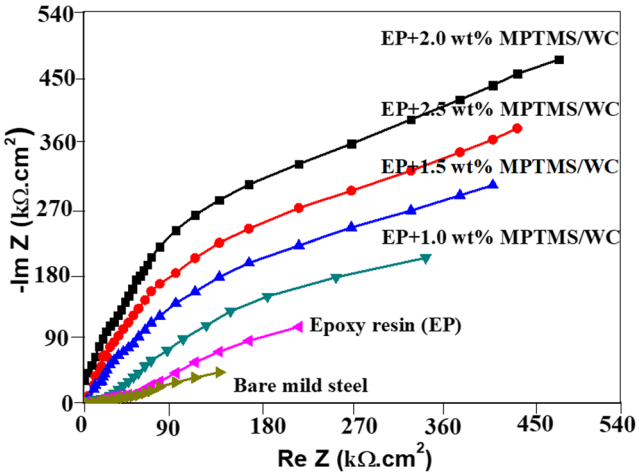

Fig. 5 Nyquist plots obtained for bare mild steel, and the mild steel coated with epoxy (EP), EP with various % of MPTMS/WC nanoparticles in chloride media

effect and the reactive nanoparticles which result in the strong adhesive strength.

3.2.2 Potentiodynamic Polarization Studies

Figure 8 demonstrates the polarization plots of (a) epoxy (EP), (b) EP-WC, (c) EP-3-mercaptopropyltrimethoxysilane (MPTMS), and (d) EP-MPTMS/WC nanocomposite coated mild steel for various exposure days in the marine environment. The resultant polarization plots are extrapolated and the extrapolated data are displayed in Table 2. The analysis of the data shows that the steel specimen coated with EP-MPTMS/WC nanocomposite exhibits reduced current density (i_{corr}) due to corrosion and least corrosion rate (*CR*). However, enhanced values of i_{corr} and *CR* are obtained for the plain EP coated specimen. This confirms the improved barrier properties of the EP-MPTMS/WC coated specimen due to the effective reaction between highly reactive nanoparticles (MPTMS/WC) and epoxy matrix. The values of i_{corr} for bare steel, epoxy (EP), EP-MPTMS, EP/WC and EP-MPTMS/WC coated specimens are found to be 09.12 μA/cm^2, 05.76 μA/cm^2, 03.17 μA/cm^2, 02.22 μA/cm^2 and 0.25 μA/cm^2, respectively when these specimens are in contact with the electrolyte for 1 h. However, these values of i_{corr} for bare steel, epoxy (EP), EP-MPTMS, EP/WC and EP-MPTMS/WC coated specimens are increased to 36.75 μA/cm^2, 12.45 μA/cm^2, 7.98 μA/cm^2, 5.65 μA/cm^2 and 0.35 μA/cm^2, respectively when these specimens are in contact with the chloride media for longer time (240 h). Moreover, higher R_p and lower corrosion rate (CR) values are obtained for bare steel (R_p: 66 kΩ.cm^2 and *CR*: 0.9496 mmpy), EP (R_p: 458 kΩ.cm^2 and *CR*: 0.1612 mmpy), EP/WC (R_p: 5576 kΩ.cm^2 and *CR*: 0.0715 mmpy), EP-MPTMS (R_p: 6356 kΩ.cm^2 and *CR*: 0. 0.0657 mmpy), and EP-MPTMS/WC (R_p: 12891 kΩ.cm^2 and *CR*: 0.0015 mmpy) coated specimens at 1 h. The values of *CR* and R_p for EP-MPTMS/WC coated specimen are slightly changed (R_p: 12654 kΩ.cm^2 and *CR*: 0.0025 mmpy) even when they are in contact with the electrolyte for the longer period (240 h).

These results show that the addition of MPTMS/WC nanoparticles to the epoxy matrix improves drastically when it is compared with other investigated coatings such as EP, EP-MPTMS and EP/WC. The reactive MPTMS/WC nanoparticles help to form a uniform and compact coating due to the cross-linking structures which impede the movements of ions towards metal-coating interface. However, drastic degradation of EP coated specimen is noticed even during the short period of exposure to the electrolytes. On the other hand, EP-MPTMS/WC coated specimen shows the least degradation behavior, even after prolonged contact with the electrolytes, thus improving the life span of the coated specimen.

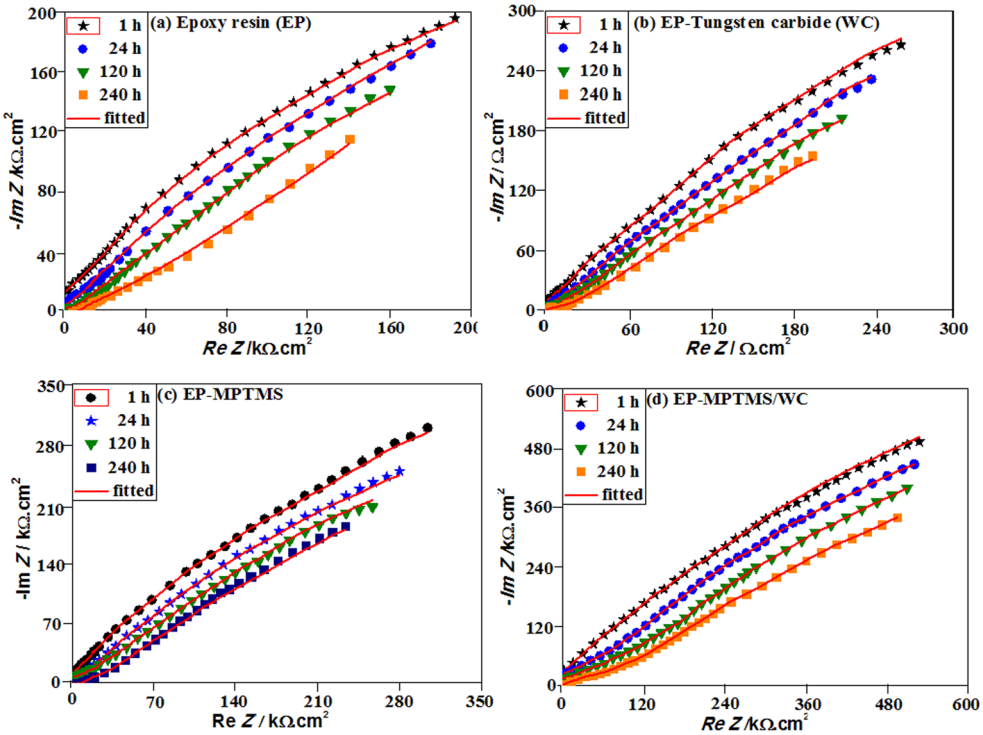

Fig. 6 Nyquist plots for of **a** epoxy (EP), **b** EP-WC, **c** EP-3-mercaptopropyltrimethoxysilane (MPTMS), and **d** EP-MPTMS/WC nanocomposite coated mild steel for various exposure times in marine environment

3.2.3 Scanning Electrochemical Spectroscopy (SECM)

Figure 9 depicts the images obtained when the SECM measurements are carried out along the scratched surface of the EP, EP-MPTMS, EP/WC and EP-MPTMS/WC coated specimen after contact with the electrolytes for 1 h and 240 h, respectively. The potential at the tip is set at +0.60 V so that the oxidation of ferrous ions to ferric ions can be noticed at this potential. The variation of color in the scratch is directly related to the dissolution of iron. Therefore, higher current is comparatively noticed in the damaged area than the undamaged area of the coated specimen. This proves that the iron is dissolved at the damaged area of the coated specimen. The degradation of Fe occurs at the metal-coating interface of the coated system [36]. The current noticed on the damaged surface of the EP coated specimen is 5.8 nA/cm^2 at 1 h and 14.9 nA/cm^2 at 15 h. The rise in degradation of iron occurs when the coated specimen is in contact with the electrolyte for a longer period (20 h). This rise in current is directly related to the degradation of iron at the metal-coating interface. However, the noticed current on the surface of the damaged EP-WC, EP-MPTMS, and EP-MPTMS/WC coated specimen is 3.9 nA/cm^2, 3.7 nA/cm^2, and 1.3 nA/cm^2, respectively after 1 h exposure. On the other hand, the noticed current on the damaged surface of the EP-MPTMS, EP/WC and EP-MPTMS/WC coated specimen is 13.5 nA, 9.3 nA and 2.4 nA, respectively after exposure to 240 h. Noticing of least current at the damaged surface of the EP-MPTMS/WC coated specimen is because of the fact that the inclusion of MPTMS/WC nanoparticles in the EP coating causes the uniform and compact structures in the coating which impedes the degradation of iron by preventing the movement of ions reaching the coating-metal interface. The passivation also helps to hinder the degradation of iron by impeding the electrolyte to reach the bare metal surface. However, noticing of high current is possible because of the pores in addition to the damage on the plain epoxy coated surface. The pores and uneven coating in EP and uneven distribution of the nanoparticles in EP-WC coating result in the increased current on the coated surface. The steel specimen is not exposed to the harsh environment

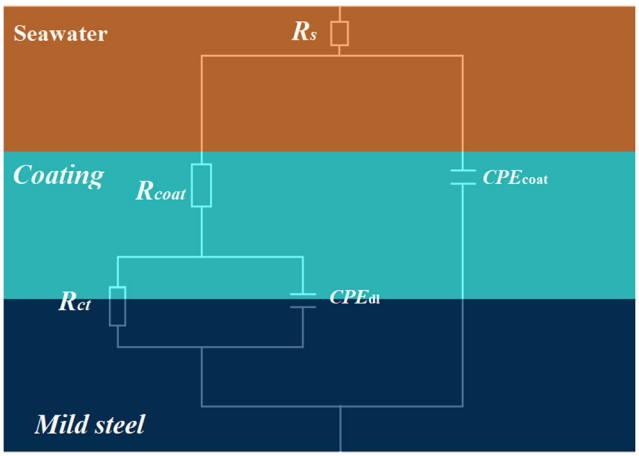

Fig. 7 Equivalent electrochemical circuit for epoxy (EP), EP-WC, EP-MPTMS, and EP-MPTMS/WC nanocomposite coated mild steel for various exposure times in seawater

Table 1 The fitted results of EIS using equivalent circuit

Sample	Time/h	R_s ($\Omega.cm^2$)	R_{coat} ($k\Omega.cm^2$)	CPE_{coat} (μF)	n_c	R_{ct} ($k\Omega.cm^2$)	CPE_{dl} (μF)	n_{dl}
Mild steel	1	119	–	–	–	65.34	552.12	0.68
	24	92	–	–	–	43.68	845.13	0.65
	120	81	–	–	–	18.60	1096.37	0.62
	240	75	–	–	–	03.96	1452.32	0.59
Epoxy (EP) coating	1	115	142.35	55.12	0.76	245.67	427.10	0.76
	24	103	84.90	100.35	0.71	195.63	645.77	0.74
	120	94	41.25	128.55	0.67	138.40	796.39	0.72
	240	85	1.11	160.36	0.66	87.12	1052.70	0.70
EP-WC Coating	1	151	2685.12	50.05	0.78	2890.46	352.80	0.84
	24	129	2298.87	80.30	0.76	2478.44	545.53	0.82
	120	118	1858.65	108.50	0.74	2099.85	696.88	0.80
	240	105	1401.33	134.20	0.72	1698.75	952.24	0.78
EP-MPTMS Coating	1	199	3056.35	39.20	0.80	3299.55	253.05	0.90
	24	183	2765.32	61.70	0.78	3001.34	354.63	0.88
	120	168	2487.43	87.27	0.76	2718.75	445.07	0.86
	240	155	2132.17	114.90	0.74	2487.41	610.10	0.84
EP-MPTMS/WC Coating	1	285	5890.65	30.60	0.84	6998.45	142.50	0.92
	24	271	5834.70	50.80	0.83	6924.55	205.25	0.91
	120	260	5765.34	70.40	0.82	6835.15	345.10	0.90
	240	255	5699.76	93.35	0.81	6754.90	396.70	0.89

Table 2 Results of potentiodynamic polarization measurements

Sample	Time/h	$-E_{corr}$ (mV)	i_{corr} ($\mu A/cm^2$)	β_a (mV/dec)	β_c (mV/dec)	R_p ($k\Omega.cm^2$)	CR (mmpy)
Mild steel	1	405	09.12	997.70	378.24	66	0.7999
	24	611	14.25	858.15	350.01	44	1.1370
	120	807	20.35	756.20	301.15	19	1.3899
	240	1070	36.75	665.70	250.20	04	1.9158
Epoxy (EP) coating	1	302	05.76	375.15	315.45	458	0.1612
	24	451	07.58	300.15	250.01	351	0.1845
	120	607	09.89	225.20	211.15	241	0.2145
	240	714	12.45	155.70	130.20	111	0.2760
EP-WC coating	1	206	03.17	248.75	239.10	5576	0.0715
	24	312	04.70	205.15	190.43	4777	0.1145
	120	417	06.25	150.20	125.75	3959	0.1512
	240	507	07.98	109.35	110.27	3100	0.1940
EP-MPTMS coating	1	151	02.22	196.12	198.96	6356	0.0657
	24	226	03.18	148.75	131.75	5766	0.0965
	120	322	04.45	125.32	90.37	5211	0.1218
	240	401	05.65	79.24	72.71	4675	0.1512
EP-MPTMS/WC coating	1	104	0.25	154.05	149.10	12,891	0.0015
	24	174	0.28	105.68	131.75	12,801	0.0018
	120	241	0.32	65.64	90.37	12,725	0.0021
	240	298	0.35	41.06	51.74	12,654	0.0025

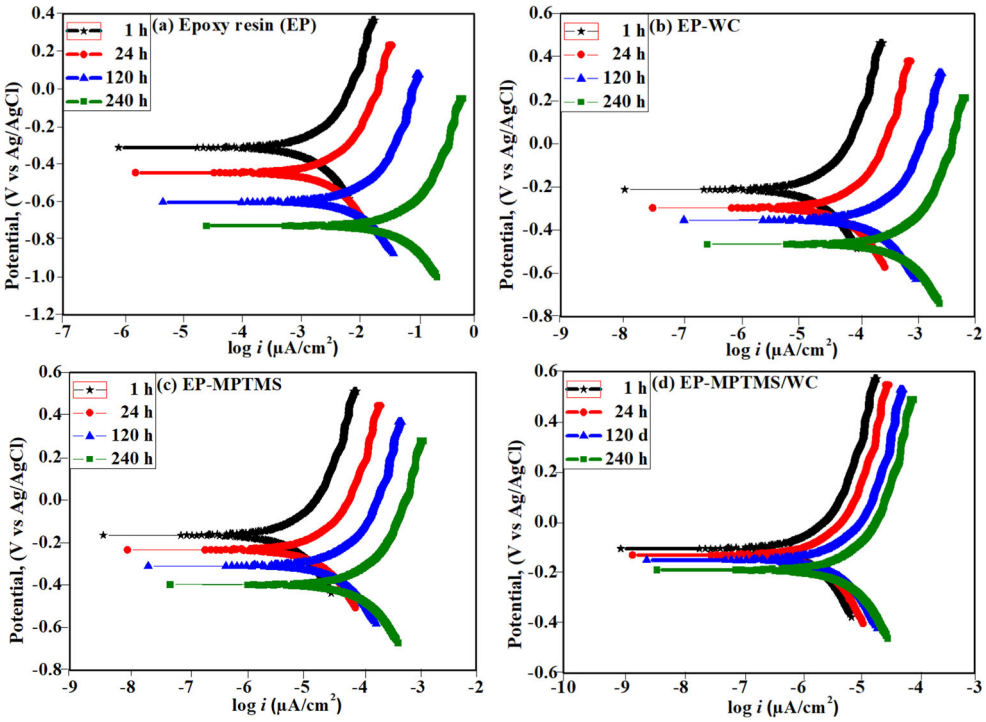

Fig. 8 Potentiodynamic polarization curves of **a** epoxy (EP), **b** EP-WC, **c** EP-MPTMS, and **d** EP-MPTMS/WC nanocomposite coated mild steel for various exposure times in seawater

when it is coated with EP-MPTMS/WC nanocomposite because the strong binding force between MPTMS/WC nanoparticles and EP and also enhanced adhesion strength of the coating to the steel surface help to decrease the corrosion rate by not allowing the electrolytes to interact with the bare steel surface. The synergistic effects between EP matrix and MPTMS and the presence of reactive nanoparticles containing amino group in the EP coating formulation prolong the life span of the EP-MPTMS/WC coating.

3.3 Surface Morphological Studies

SEM/EDX analyses (cross-sectional) of the EP, EP-MPTMS, EP-WC and EP-MPTMS/WC coated steel after 240 h of contact with the electrolytes are shown in Fig. 10 (a-h). Extensive degradation is clearly visible in the case of EP coated specimen (Fig. 10a) due to high porous and non-uniform nature of EP coating. However, in the case of the EP-MPTMS coated specimen, the degradation is somewhat reduced due to the synergistic effect between MPTMS and EP matrix. The crack is formed because of the ineffective binding strength. The aggressive ions are moved through the cracks reaching the metal surface. In the case of the EP-WC coated specimen, the aggregation of WC nanoparticles in the EP matrix forms the pores through which electrolytes could be penetrated reaching the coating-metal interface. In the case of the EP-MPTMS/WC coating, uniform coating without pores and cracks is clearly seen. This is due to the compact cross-linked structure formed between the reactive MPTMS/WC and the EP matrix. This creates the complicated pathways for the electrolytes to reach the bare metal surface. The presence of C, O, and Fe elements in the EDX analyzes of coated specimen confirm that the EP matrix is involved in the entire steel coated specimen. However, the percentage of iron emerging from the degradation products is varied for each coating. The higher amount of iron is detected for the plain EP coated specimen. On the other hand, least amount of iron is found for the EP-MPTMS/WC coated specimen, which contains W, Si and S apart from C, and O. The compact cross-linked structure between MPTMS/WC and the EP matrix helps to increase the life span of the coated specimen without degradation. The MPTMS/WC enhances the binding strength of the EP coated system, which help to hinder the ion movement reaching the bare steel surface. Moreover, the Fe percentage is rapidly reduced for EP-MPTMS/WC compared to pure EP coating to the sample. This is confirmed that the presence of modified EP-MPTMS/WC coating form a better binding to the metal surface which could resist the degradation process.

XRD analyses were accomplished on the degradation products of the EP, EP-MPTMS, EP/WC and EP-MPTMS/WC coated steel specimen after 240 h of contact with the electrolytes. This test was carried out in a 2θ range of 20 to 70 degrees and the resultant XRD patterns are given in Fig. 11. XRD patterns of the steel coated specimen are consisting of F_3O_4, γ-FeOOH, and Fe. The peaks corresponding to γ-FeOOH, Fe_3O_4 and Fe and their intensities are appeared to be higher for the plain EP coated steel specimen. In the case of the EP-MPTMS/WC coated steel specimen, the XRD patterns also show the same peaks relating to γ-FeOOH, Fe and

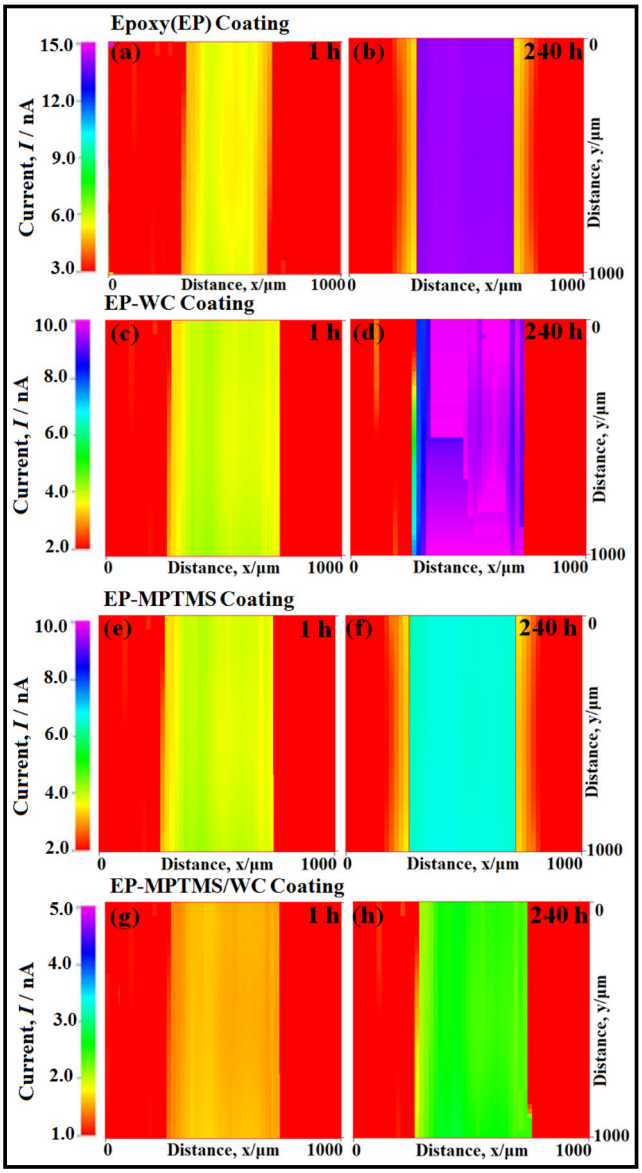

Fig. 9 SECM analysis of epoxy (EP) (**a** and **b**), EP-WC (**c** and **d**),EP-MPTMS (**e** and **f**), and EP-MPTMS/WC (**g** and **h**) nanocomposite coated mild steel for 1 h and 240 h of immersion in seawater at tip potential +0.60 V vs. Ag/AgCl/KCl reference electrode

Fe_3O_4, but with much reduced intensity compared to EP coated specimen. A considerable reduction in the peak at 240 h of immersion is due to the inhibition of corrosion process. The passive layered peaks obtained at 35.85° and 48.44° corresponding to MPTMS reinforced WC nanoparticles. The reactive MPTMS/WC nanoparticles play a major role in preventing the degradation processes of the EP-MPTMS/WC coated system.

3.4 Permeability Test

Figure 12a displays the results of the permeable nature of the oxygen in the EP, EP-MPTMS, EP/WC and EP-MPTMS/WC coatings before and after several days of contact with the electrolytes. The results show very low penetrability of O_2 gas for the EP-MPTMS/WC coating due to the addition of MPTMS/WC in EP matrix which significantly covers the pores/cracks through which the O_2 gas cannot be penetrated. The ability of the O_2 gas to pass through the EP-MPTMS/WC is drastically restricted because the thin passive layer by MPTMS/WC protects the surface from harsh environments. However, an increased movement of O_2 through the EP coating is possible due to pores and cracks. Hence, MPTMS/WC embedded EP coating shows an excellent O_2 gas barrier property.

Figure 12b represents the results of permeable nature of water in the EP, EP-WC, EP-MPTMS, and EP-MPTMS/WC coatings before and after several of contact with the electrolytes. It is evident from the results that least penetration of water is displayed by EP-MPTMS/WC coatings because of the reinforcement of MPTMS/WC in the EP, which repels the absorbing ability of water by forming MPTMS/WC layer that protects the coated specimen. It leads to reduction in the initiation of the degradation process. However, the degradation processes are enhanced for EP coated specimen due to non-uniform coating. Therefore, EP-MPTMS/WC coating demonstrates superior barrier properties against water and oxygen.

3.5 Mechanical Studies

The effect of adhesion strength after the introducing MPTMS/WC in the EP coatings was investigated by Pull-off adhesion tests and the resultant data were presented in Fig. 13a. The test was carried out before and after several days of contact with the electrolytes for pure EP, EP/WC, EP-MPTMS, and EP-MPTMS/WC coatings. The pure EP adhesion strength is declined quickly to 1.2 MPa from 6.0 MPa after 240 h of contact with electrolytes because of the presence of pores and cracks on the coating. However, the adhesion strength of the EP-MPTMS/WC nanocomposite coatings is found to be very high (12.5 MPa) compared to the pure EP (6.0 MPa), EP-MPTMS (9.1 MPa) and EP-WC (9.5 MPa) without the exposure to the electrolyte and the value of adhesion strength of the EP-MPTMS/WC nanocomposite reaches only 11.2 MPa even after 240 h of exposure to the electrolytes. The main reason for the enhanced adhesion strength is due to higher interfacial interaction between EP and MPTMS/WC nanoparticles. Therefore, it is confirmed that EP-MPTMS/WC coating demonstrates superior adhesive property among the investigated coatings.

Figure 13b displays the results of the hardness testing of the EP, EP-MPTMS, EP-WC and EP-MPTMS/WC coatings before and after several days of contact with the electrolytes. The value of hardness for pure EP coating reaches only 290 MPa and declines to a very low value of 80 MPa after 240 h of exposure to the electrolytes due to the weak adhesive strength

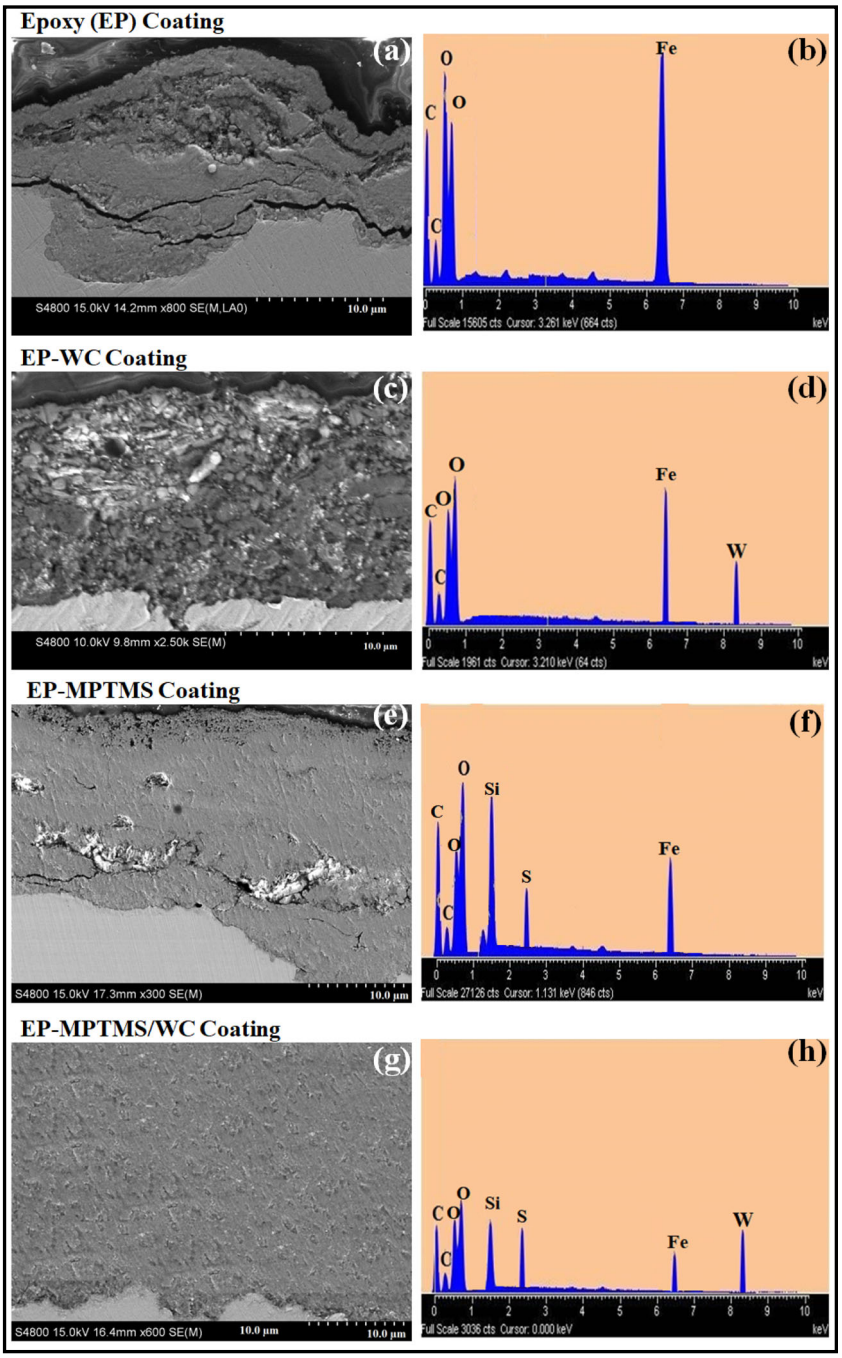

Fig. 10 SEM/EDX analyses (Cross-sectional) of epoxy (EP), EP-WC, EP-MPTMS, and EP-MPTMS/WC nanocomposite coated mild steel after 240 h of immersion in seawater

of EP coating. However, the value of hardness for EP-MPTMS/WC coating reaches 1150 MPa and declines very slowly and reaches 1050 MPa even after prolonged exposure to the electrolytes. This is possible because of the introduction of reactive MPTMS/WC nanoparticles in EP coatings which enhances the hardness value by creating the cross-linking structure between MPTMS/WC and EP resulting in the synergistic effects. Hence, EP-MPTMS/WC coating demonstrates superior hardness property among the investigated coatings.

Figure 13c shows the values of tensile strength of EP, EP-MPTMS, EP-WC and EP-MPTMS/WC coatings before and after several days of contact with the electrolytes. The value of tensile strength for EP is found to be 69 MPa and reaches very low value of 24 MPa after exposure to the electrolytes. This confirms the very low resistive property of the EP coating. However, the tensile strength for EP–MPTMS/WC coating shows an enhanced value of 160 MPa and its value declines very slowly and reaches 142 MPa even after pronged exposure to the electrolyte. The reactive MPTMS/WC

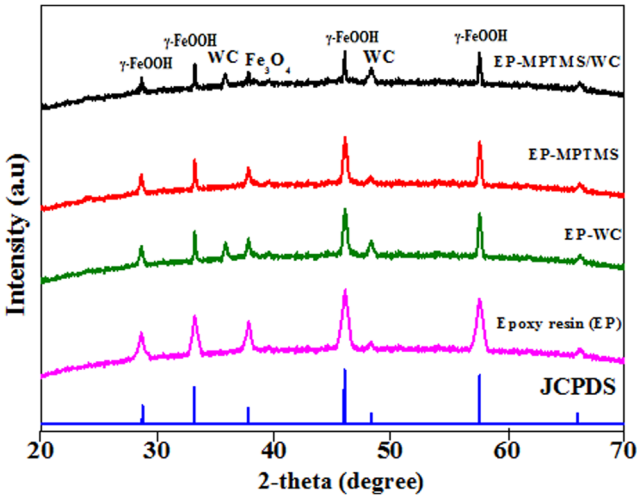

Fig. 11 XRD patterns of epoxy (EP), EP-WC, EP-MPTMS, and EP-MPTMS/WC nanocomposite coated mild steel after 240 h of immersion in seawater

nanoparticles act like a barrier film that protects the steel surface from degradation. Therefore, EP-MPTMS/WC shows superior tensile strength among the investigated coatings.

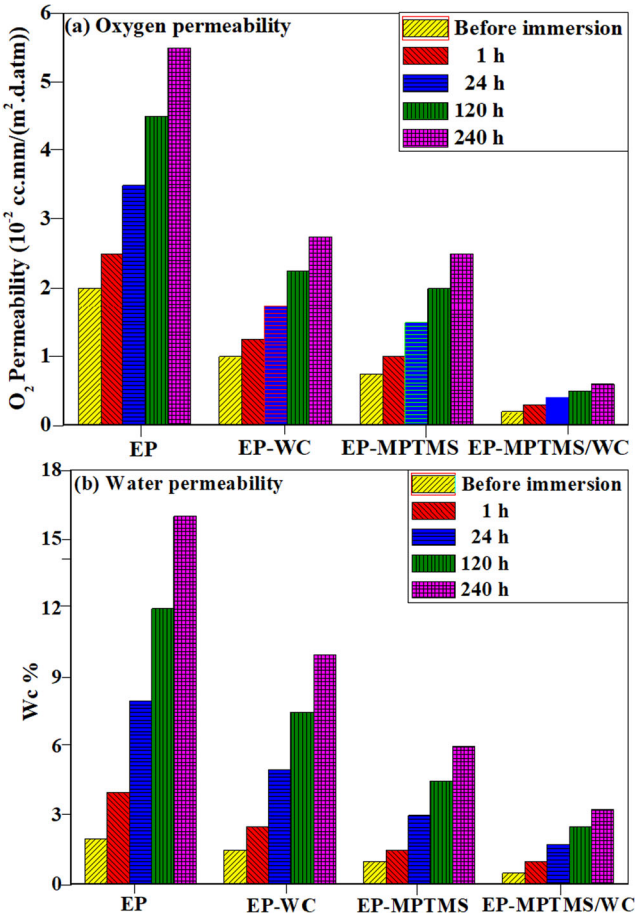

Fig. 12 The permeability investigation of **a** oxygen and **b** water for epoxy (EP), EP-WC, EP-MPTMS, and EP-MPTMS/WC coated mild steel for various times of exposure to the electrolyte

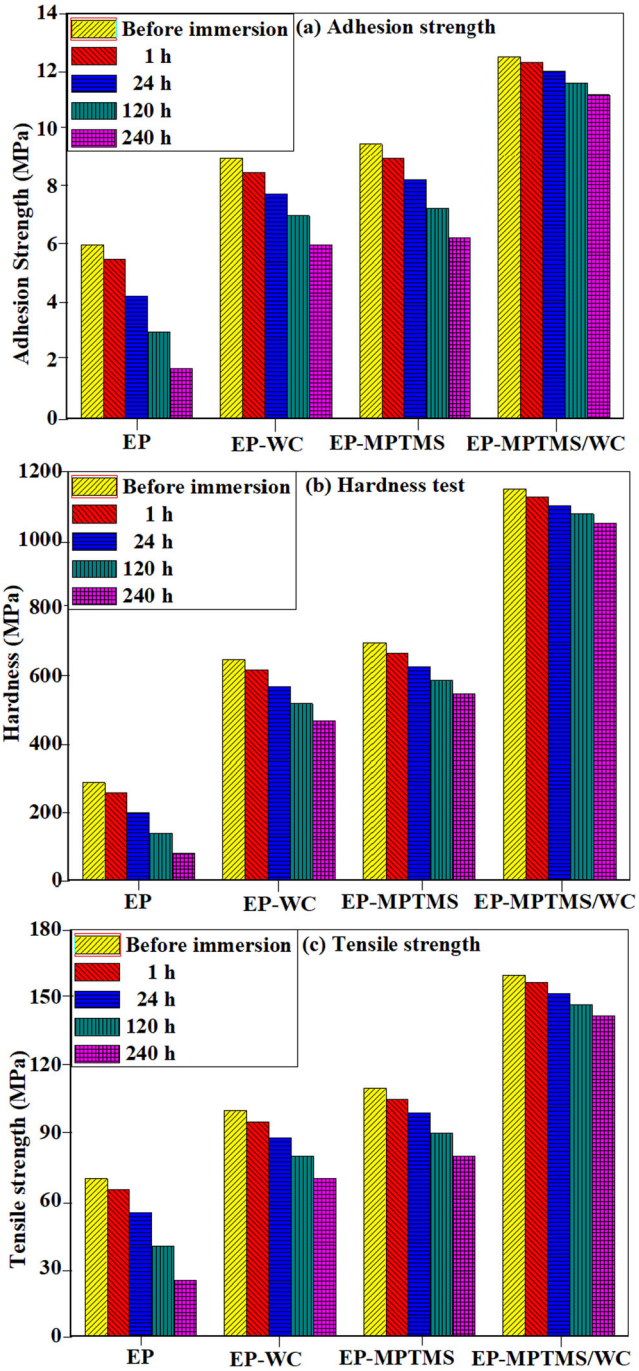

Fig. 13 The results of **a** adhesion strength, **b** hardness, and **c** tensile strength data of mild steel coated with epoxy (EP), EP-WC, EP-MPTMS, and EP-MPTMS/WC before and after immersion in seawater for 1, 24, 120 and 240 h

3.6 Water Contact Angle Measurements

Water contact angle measurements were carried out in order to get information about the investigated coatings, whether they are hydrophilic or hydrophobic. Hydrophobic property confirms the barrier abilities of the coatings. Water contact angle measurements for (a) epoxy (EP), (b) EP-WC, (c) EP-

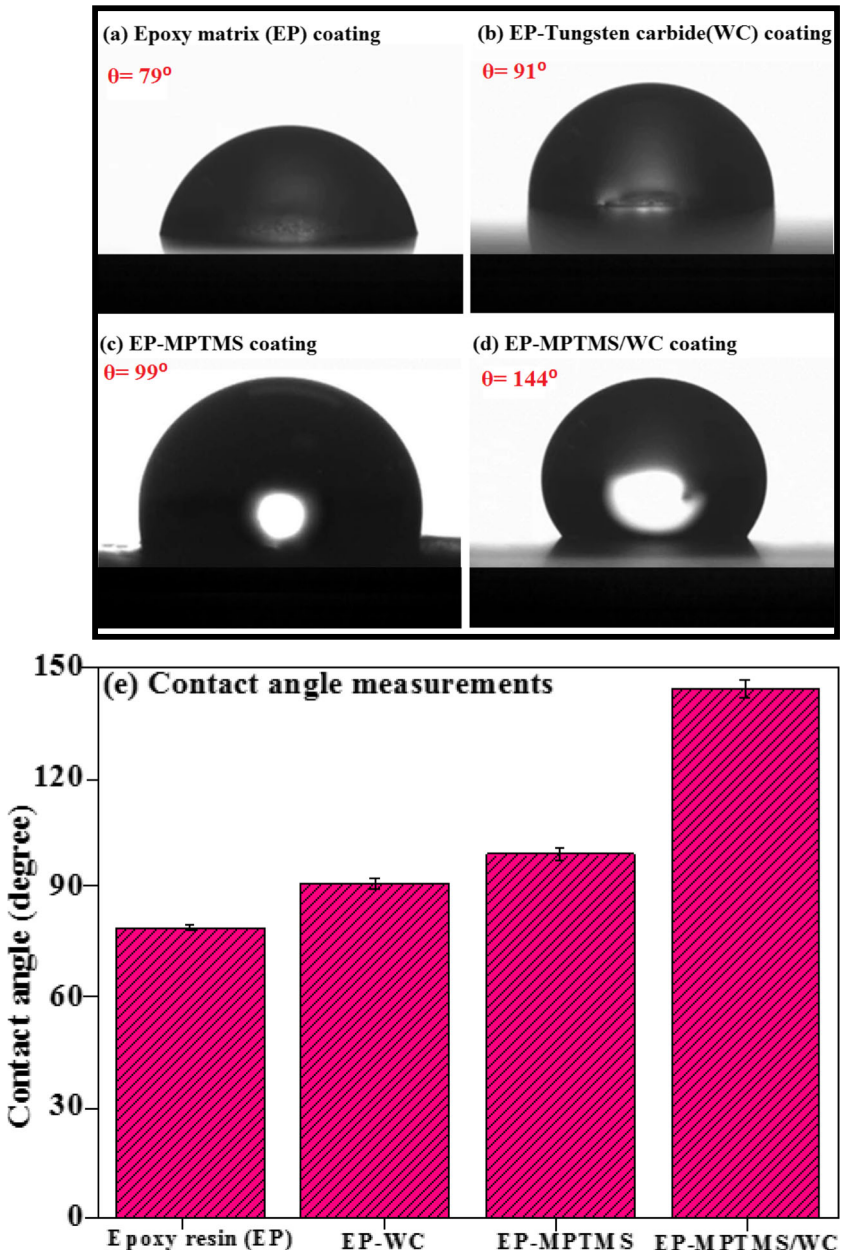

Fig. 14 Water contact angle measurements for **a** epoxy (EP), **b** EP-WC, **c** EP-3-mercaptopropyltrimethoxysilane (MPTMS), and **d** EP-MPTMS/WC nanocomposite coated mild steel and **e** histogram of a, b, c, and d

MPTMS, and (d) EP-MPTMS/WC nanocomposite coated mild steel and (e) histogram of a, b, c, and d. are presented in Fig. 14. The values of contact angles for epoxy (EP), EP-WC, EP-MPTMS, and EP-MPTMS/WC are found to be 79°, 91°, 99°, and 144°, respectively. The surface is said to be hydrophilic if the angle value is less than 90, and if the value is greater than 90, it is said to be hydrophobic [37, 38]. Therefore, it is confirmed that the EP-MPTMS/WC coated surface shows superior hydrophobic property which demonstrates superior barrier properties among the investigated coatings. However, EP, EP-MPTMS, and EP-WC coated surface show hydrophilic property. These results compliment other results of the investigated coatings.

4 Conclusion

The novel EP, EP-MPTMS, EP/ WC, and EP-MPTMS/WC coated mild steel samples were prepared and investigated extensively by employing several characterization techniques in natural seawater. XRD patterns confirmed complete surface modification of WC nanoparticles by MPTMS in which there was no drastic change in the structures. The presence of N, O and C in MPTMS/WC nanoparticles proved that WC was embedded with MPTMS. The resulting coated specimens were evaluated by EIS, potentiodynamic polarization, SECM, SEM/EDX, contact angle, and XRD techniques. The EIS studies revealed superior coating and charge transfer

resistances by EP-MPTMS/WC coating (R_{coat}: 5890.65 kΩ.cm^2 and R_{ct}: 6998.45 kΩ.cm^2) which was much higher than the EP coated specimen. Similarly, polarization studies demonstrated the much reduced i_{corr} value was observed for EP-MPTMS/WC coating (0.15 μA/cm^2) whereas; much higher i_{corr} value was obtained for EP coating (5.76 μA/cm$_2$). These results confirm the superior barrier properties of the EP-MPTMS/WC coating due to the introduction MPTMS/WC nanoparticles in EP matrix which produces compact cross-linking structures which prevent the degradation of the coatings. The results of SECM studies also compliment the EIS and polarization studies. Mechanical studies revealed the superior adhesion strength, hardness and tensile strength for the EP-MPTMS/WC coatings among the investigated coatings. The penetrating ability of oxygen and water has been drastically reduced for the EP-MPTMS/WC coatings. In addition to this, contact angle of 144° is observed for the EP-MPTMS/WC coating which is proved to be super hydrophobic nature of the EP-MPTMS/WC coating. Hence, the modified novel EP-MPTMS/WC nanocomposite exhibits superior barrier, mechanical and hydrophobic properties than other investigated coatings. Therefore, the EP-MPTMS/WC coating could be used as a potential coating material for the industrial applications in the marine environments. This work can be extended in detail by incorporating different functionalized nanoparticles in the epoxy matrix with varying temperatures so that it could be used as a potential coating material for brass used in the cooling water system.

Acknowledgements Not applicable.

Author Contribution Joseph Raj Xavier: Visualization, Conceptualization, Methodology, Resources, Validation, Formal analysis, Investigation, Writing – original draft, Writing – review & editing.

Funding No funding was received to assist with the preparation of this manuscript.

Data Availability The datasets generated during and/or analyzed during the current study are available from the corresponding author on reasonable request.

Declarations

Ethics Approval Not applicable (The results of this study do not involve any human or animal).

Consent to Participate Not applicable (The results of this study do not involve any human or animal).

Consent for Publication Not applicable (The results of this study do not involve any human or animal).

Competing Interests The author declares that he has no known competing financial interests or personal relationships that could have appeared to influence the work reported in this paper.

References

1. Vinodhini SP, Joseph Raj X (2021) Investigation of anticorrosion and mechanical properties of azole functionalized graphene oxide encapsulated epoxy coatings on mild steel. J Fail Anal Preven 21: 649–661
2. Elemike EE, Nwankwo HU, Onwudiwe DC (2019) Synthesis and comparative study on the anti-corrosion potentials of some Schiff base compounds bearing similar backbone. J Mol Liq 276:233–242
3. Mo R, Hu J, Huang H, Sheng X, Zhang X (2019) Tunable, self-healing and corrosion inhibiting dynamic epoxy-polyimine network built by post-crosslinking. J Mater Chem A 7:3031–3038
4. Khan R, Azhar MR, Anis A, Alam MA, Boumaza M, Al-Zahrani SM (2016) Facile synthesis of epoxy nanocomposite coatings using inorganic nanoparticles for enhanced thermo-mechanical properties: a comparative study. J Coat Technol Res 13:159–169
5. Alagi P, Ghorpade R, Choi Y, Patil U, Kim I, Baik J et al (2017) Carbon dioxide-based polyols as sustainable feedstock of thermoplastic polyurethane for corrosion-resistant metal coating. ACS Sustain Chem Eng 5:3871–3881
6. Pathan S, Ahmad S (2013) s-Triazine ring–modified waterborne alkyd: synthesis, characterization, antibacterial and electrochemical corrosion studies. ACS Sustain Chem Eng 1:1246–1257
7. Cao M, Wang H, Cai R, Ge Q, Jiang S, Zhai L, Jiang S (2015) Preparation and properties of epoxy-modified tung oil waterborne insulation varnish. J Appl Polym Sci 132:42755
8. Kumar S, Krishnan S, Samal S, Mohanty S, Nayak S (2017) Itaconic acid used as a versatile building block for the synthesis of renewable resource-based resins and polyesters for future prospective: a review. Polym Int 66:1349–1363
9. Boubakri A, Guermazi N, Elleuch K, Ayedi H (2010) Study of UV aging of thermoplastic polyurethane material. Mat Sci Eng A 527: 1649–1654
10. Huang T, Wang Y, Hsieh K, Lin J (2012) Molecular-level dispersion of phosphazene-clay hybrids in polyurethane and synergistic influences on thermal and UV resistance. Polymer 53:4060–4068
11. Ma C, Xu L, Xu W, Zhang G (2013) Degradable polyurethane for marine anti-biofouling. J Mater Chem B 1:3099–3106
12. Muhammad R, Mohammad D, Saidatul S (2014) Development of vegetable-oil-based polymers. J Appl Polym Sci 131:1–13
13. Pradhan S, Pandey P, Mohanty S, Nayak S (2016) Insight on the chemistry of epoxy and its curing for coating applications: a detailed investigation and future perspectives. Polym Plast Technol 55:862–877
14. Ammar S, Ramesh K, Vengadaesvaran B, Ramesh S, Arof A (2016b) Amelioration of anticorrosion and hydrophobic properties of epoxy/PDMS composite coatings containing nano ZnO particles. Prog Org Coat 92:54–65
15. Xavier JR (2021) Corrosion protection performance and interfacial interactions of polythiophene/silanes/MnO2 nanocomposite coatings on magnesium alloy in marine environment. Int J Polym Anal 26:309–329
16. Xavier JR (2021) Electrochemical and dynamic mechanical studies of newly synthesized polyurethane/SiO_2-Al_2O_3 mixed oxide nanocomposite coated steel immersed in 3.5% NaCl solution. Surf Interfaces 22:100848. https://doi.org/10.1016/j.surfin.2020.100848
17. Zheng S, Bellido-Aguilar DA, Huang Y, Zeng X, Zhang Q, Chen Z (2019) Mechanically robust hydrophobic bio-based epoxy coatings for anti-corrosion application. Surf Coat Technol 363:43–50. https://doi.org/10.1016/j.surfcoat.2019.02.020
18. Xavier JR (2021) Improvement of mechanical and anticorrosion coating properties in conducting polymer poly (propyl methacrylate) embedded with silane functionalized silica nanoparticles. Silicon 13:3291–3305

19. Atta AM, Mohamed NH, Rostom M, Al-Lohedan HA, Abdullah MM (2019) New hydrophobic silica nanoparticles capped with petroleum paraffin wax embedded in epoxy networks as multifunctional steel epoxy coatings. Prog Org Coat 128:99–111
20. Xavier JR (2021) Electrochemical and mechanical investigation of newly synthesized NiO-ZrO_2 nanoparticle–grafted polyurethane nanocomposite coating on mild steel in chloride media. J Materi Eng Perform 30:1554–1566
21. Ghosal A, Rahman OU, Ahmad S (2015) High-performance soya polyurethane networked silica hybrid nanocomposite coatings. Ind Eng Chem Res 54:12770–12787
22. Xavier JR (2022) Novel multilayer epoxy nanocomposite coatings for superior hydrophobic, mechanical and corrosion protection properties of steel. Diam Relat Mater 123:108882
23. Shi H, Liu F, Yang L, Han E (2008) Characterization of protective performance of epoxy reinforced with nanometer-sized WC and SiO_2. Prog Org Coat 62:359–368
24. Fadl A, Abdou M, Hamza M, Sadeek S (2020) Corrosion-inhibiting, self-healing, mechanical-resistant, chemically and UV stable PDMAS/WC epoxy hybrid nanocomposite coating for steel petroleum tanker trucks. Prog Org Coat 146:105715
25. Radoman TS, Dzunuzovic JV, Jeremic KB, Grgur BN, Milicevic DS, Popovic IG, Dzunuzovic ES (2014) Improvement of epoxy resin properties by incorporation of WC nanoparticles surface modified with gallic acid esters. Mater Des 62:158–167
26. Ying L, Wu Y, Nie C, Wu C, Wang G (2021) Improvement of the tribological properties and corrosion resistance of epoxy-PTFE composite coating by nanoparticle modification. Coatings 11(10): 1–12
27. Xavier JR (2020) Electrochemical, mechanical and adhesive properties of surface modified NiO-epoxy nanocomposite coatings on mild steel. Mater Sci Eng B 260:114639
28. Xavier JR (2021) Dynamic mechanical and electrochemical analysis of newly synthesized polyurethane/CuO–NiO mixed metal oxide nanocomposite coated steel in 3.5% NaCl solution. Prot Met Phys Chem Surf 57:984–994
29. Hu C, Li Y, Zhang N, Ding Y (2017) Synthesis and characterization of a poly(oanisidine)- SiC composite and its application for corrosion protection of steel. RSC Adv 7:11732–11742
30. Ch H, Qing Y, Li Y, Zhang N (2017) Preparation of poly(o-ethoxyaniline)-nano SiC composite and evaluation of its corrosion resistance properties. J Alloys Compd 717:98–107
31. Vinodhini SP, Joseph Raj X (2021) Evaluation of newly synthesized multifunctional nanocomposite coated cupronickel alloy in marine environment. Mater Chem Phys 268:124721
32. Zhao J, Milanova M, Warmoeskerken MMCG, Dutschk V (2012) Surface modification of WC nanoparticles with silane coupling agents. Colloids Surf A Physicochem Eng Asp 413:273–279
33. Wang N, Wanlu F, Zhang J, Li X, Fang Q (2015) Corrosion performance of waterborne epoxy coatings containing polyethylenimine treated mesoporous-WC nanoparticles on mildsteel. Prog Org Coat 89:114–122
34. Wu Y, Dang J, Lv Z, Zhang R (2018) The preparation of tungsten carbides and tungsten powders by reaction of tungsten trioxide with methanol. Int J Refract Met Hard Mater 76:99–107
35. Raja Beryl J, Joseph Raj X (2021) A study on the anticorrosion performance of epoxy nanocomposite coatings containing epoxy-silane treated nanoclay on mild steel in chloride environment. J Polym Res 28:189
36. Joseph Raj X, Raja Beryl J, Vinodhini SP, Boomadevi Janaki G (2021) Enhanced protective and mechanical properties of Polypyrrole coatings modified by Silane/CoO nanocomposite on AZ91 Mg alloy in chloride media. J Bio-Tribo-Corros 7:46
37. Park EJ, Yoon HS, Kim DH, Kim YH, Kim YD (2014) Preparation of self-cleaning surfaces with a dual functionality of superhydrophobicity and photocatalytic activity. Appl Surf Sci 319:367–371
38. Raja Beryl J, Xavier JR (2021) Influence of silane functionalized nanoclay on the barrier, mechanical and hydrophobic properties by clay nanocomposite films in an aggressive chloride medium. Colloids Surf A Physicochem Eng Asp 630:127625
39. Xavier JR, Nallaiyan R (2016) Application of EIS and SECM studies for investigation of anticorrosion properties of epoxy coatings containing ZrO_2 nanoparticles on mild steel in 3.5% NaCl solution. J Fail Anal Prev 16:1082–1091
40. Dana H, Abdeen MEH, Koc M, Muataz A, Atieh A (2019) Review on the corrosion behaviour of nanocoatings on metallic substrates. Materials 12(210):1–42